Complexity Project
The Oslo Model

CID: 01888850

21 February 2022

Abstract: Complexity systems can be found in a variety of disciplines, and researchers use the theory of complexity science to study topics such as earthquakes and the emergent properties of cities. An interesting property of some complex systems is self-organized criticality, and we study it here using the Oslo model. We look at the average heights of piles of fixed system sizes and their associated avalanche-size distributions. We then collapse the data by making use of the scaling property of the normalized-probability distributions to confirm the finite-size scaling ansatz. Finally, we measure the moments of the probability densities and estimate error bars. This analysis allows us to conclude that the piles studied display self-organization around a critical point corresponding to the attractor of the system dynamics.

Word count: 2487 words in report (excluding front page, figure captions, table captions, acknowledgement and bibliography).

Introduction

An interesting property displayed by some complex systems is self-organized criticality. This process involves a slowly-driven equilibrium system which self-organizes into a steady state. The critical nature of the system means its response does not depend on the magnitude of the perturbation. As grains are added to the system, threshold slopes are breached, causing avalanches. Eventually, the system experiences avalanches spanning orders of magnitude as the potential energy of added grains is converted to kinetic energy, allowing energy to dissipate out.

We would like to study such behaviors and turn to the Oslo model to do so, due to its simple, non-trivial behavior. We begin with an empty configuration where all local slopes are set to 0 and threshold slopes are 1 or 2. These local slopes are our dynamical variables and the threshold slopes account for the necessary degree of freedom. Next, we drive the system by gradually add grains to a pile. The system is relaxed if a local slope exceeds the threshold slope at that site, and new threshold slopes selected for relaxed sites only. This is repeated until all supercritical sites are relaxed.

Once the system dynamics reach the statistically stationary state, the system transitions from transient to recurrent configurations. This occurs at the crossover time t_c, defined as the point at which the number of grains added to the system is equal to the number leaving it. The Oslo-model self-organizes to this critical state, the attractor of the dynamics.

1 Implementation of the Oslo model

We implement the algorithm of the Oslo model in `Python 3.9` and test it using the `unittest` framework. The implementation also makes use of the Abelian nature of the Oslo model by relaxing supercritical sites, that is those sites for which $z_i > z_i^{th}$, via a non-ordered list. This is important as it allows for a more straightforward implementation.

We perform various tests to ensure the algorithm behaves as expected. For example, we check threshold slopes are chosen with equal probability by generating a pile $P(L = 25)$ and checking that, on average, the associated threshold slopes 1 and 2 are equally likely to appear. A natural question arises: given a stable configuration, will threshold slopes appear with equal probability? The Abelian property of the Olso model means the site relaxations commute, and since the (non-uniform) avalanche size distribution depends on the probability distribution of the threshold slopes [1], we can conclude the stable configuration does not imply thresholds will appear with equal probability.

1.1 Simple tests of the implementation

In addition to the test of threshold slopes above, we check a different set of probabilities would produce different results; for example, in the regime where 2 is chosen all of the time.

It could also be useful to verify the only values that appear in the list of threshold slopes are those which are allowed in our algorithm, i.e. 1 or 2. We do so by returning the set of unique values in the threshold slopes of a pile, and see that it is $\{1, 2\}$.

We now proceed to implementing the tests suggested in the project guidelines. We measure the height at site $i = 1$ averaged over time once the systems has reached the steady state, finding $\langle h(t = 5000, L = 16)\rangle = 26.4482$ and $\langle h(t = 15000, L = 32)\rangle = 53.8889$. We can compute the standard error to see how good of an approximation this is: $S.E. = \frac{\sigma_(h=16)}{n} = 0.038$ and $S.E. = \frac{\sigma_(h=32)}{n} = 0.046$. We find the algorithm implementation behaves as desired.

2 The height of the pile $h(t; L)$

We begin from an empty system configuration and measure the height of the piles as a function of time t, which is defined by the number of grains added to the pile. The piles are of fixed lengths, L = 4, 8, 16, 32, 64, 128, 256. Using the local slope definition $z_i = h_i - h_{i+1}$ with boundary $h_{L+1} = 0$, we can express the height of the pile as $h(t; L) = \sum_{i=1}^{L} z_i(t)$. Though this is a satisfactory definition, we will make use of the fact that the value of the sum changes if and only if there is an avalanche in the system to write more efficient code. In particular, rather than calculating the set of local slopes and summing over i, we find the height by checking how many grains have been added to or toppled from the first site in the lattice.

2.1 Plotting height $h(t; L)$ as a function of t

We generate the piles over 200,000 grain additions. From this, we measure the point at which piles reach a steady state configuration for each system size and find the height of the pile goes as the power law with respect to time. Figure 1 shows the cross-over time at which the piles adjust from transient to recurrent configurations.

In particular, the curve of pile heights eventually reaches a horizontal asymptote after which the number of grains added to the pile is the same as the number leaving it. This is useful for inferring the behavior of the dynamics of the attractors of the systems, in particular as it suggests the piles are experiencing self-organized criticality. It is clear from Figure 1 that each pile undergoes a phase transition where it switches from transient to recurrent configurations, and notably the height at which it does so scales linearly with system size: $h_r(L) \propto L$.

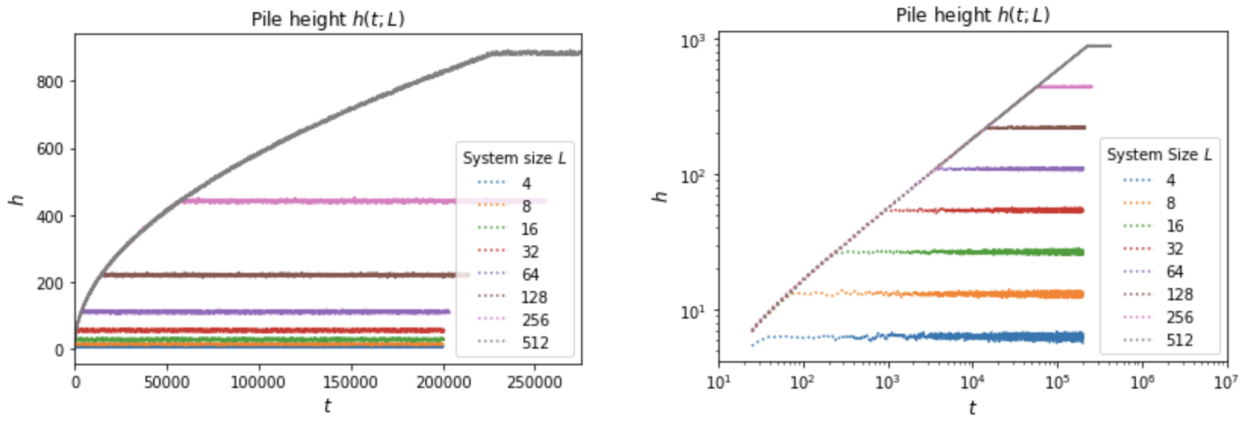

Figure 1: We plot the evolution of piles heights $P(h; L)$ for various system sizes over both a regular and log-log scale. The system size L corresponds to the number of grains in the bottom rung of the pile. We see that the height of the pile grows with an increase in system size.

2.2 Numerical measurement of average cross-over time $\langle t_c(L) \rangle$ and analysis

Now, we turn our attention to the relationship between cross-over time $t_c(L)$ and system size L. In order to estimate $\langle t_c(L) \rangle$ numerically, we calculate a moving average of the height data over range of time values, given by $\tilde{h}(t; L) = \frac{1}{M} \sum_{j=1}^{M} h^j(t; L)$, where $h^j(t; L)$ is the height at time t in the jth realisation of a system of size L. This corresponds to tracking the behavior of the system up to the point at which new grains do not change its behavior, i.e. the cross-over heights and times. Results are plotted over a log-log scale and scaling inferred: $\langle t_c(L) \rangle \propto L^2$ for $L \gg 1$.

2.3 Theoretical argument for $\langle h \rangle$ and $\langle t_c(L) \rangle$ scaling behavior

We work in the limit where $L \gg 1$ and ignore potential corrections to scaling to explore the scaling behavior of $\langle h \rangle$ and $\langle t_c(L) \rangle$. Given $L \gg 1$, for each pile we have $\langle z \rangle = \langle z_i(t) \rangle$, i.e. that the local average slope at a given time is the same as the average slope of the whole pile. The individual z_i do not depend on L because the same algorithm is run for all system sizes. We recall the definition $h(t; L) = \sum_{i=1}^{L} z_i(t)$, and derive the following:

$$\langle h(t; L) \rangle = \langle \sum_{i=1}^{L} z_i(t) \rangle = \sum_{i=1}^{L} \langle z_i(t) \rangle = \sum_{i=1}^{L} \langle z \rangle = L \cdot \langle z \rangle \propto L \tag{1}$$

As expected, the average of the height of the pile over time scales linearly with system size. Recall the definition for average cross-over time, $t_c(L) = \sum_{i=1}^{L} z_i \cdot i$. We have that,

$$\langle t_c(L) \rangle = \langle \sum_{i=1}^{L} z_i \cdot i \rangle = \sum_{i=1}^{L} \langle z \rangle \cdot i = \langle z \rangle \sum_{i=1}^{L} i$$

To continue, we use the formula for a Gaussian sum,

$$\langle z \rangle \sum_{i=1}^{L} i = \langle z \rangle \frac{L}{2}(L+1) = L^2(\frac{1}{2} + \frac{1}{2L})\langle z \rangle \propto L^2, \tag{2}$$

which we identify with the numerical estimate for scaling behavior detailed above.

2.4 Data collapse and scaling function $\mathcal{F}$

The smoothed height data is used to reduce statistical noise and make data collapse more intuitive. The data is rescaled using the proportionality relationships determined previously, as seen on the axes of Figure 2. The resulting data collapse is very exciting as it shows behavior typical of a critical system. As such, we would expect it to have an associated scaling function $\mathcal{F}$(x) whose argument and coefficient describe the dynamics of the system.

We find that indeed there is such a scaling function,

$$\tilde{h}(t; L) = L\mathcal{F}\left(\frac{t}{L^2}\right), \tag{3}$$

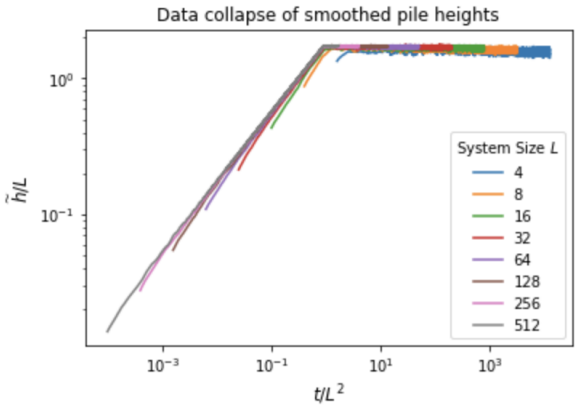

Figure 2: Data is smoothed using a moving average and collapsed over axes rescaled by the coefficient and argument of the scaling function F. The result exhibits characteristic behavior of a critical system.

where we have identified the coefficient as L and the argument as t/L^2. From the graph of the data collapse, we can easily see there is a point at which the scaling function $\mathcal{F}$ undergoes a transition from power law to constant behavior. Specifically, the mathematical discontinuity in the plot corresponds to a phase transition for the dynamics of the attractor. This can be expressed mathematically as, for $x < 1, \mathcal{F}(x)$ exhibits power law behavior and for $x \geq 1, \mathcal{F}(x)$ is a constant function in x. In the case of the Olso model, this describes the transition to a steady state configuration for which the average number of grains introduced into the system equals the average number of grains toppling out.

2.4.1 Inferring transient state behavior of $\tilde{h}(t; L)$

We have identified the power law behavior in the graph and use it to fit the data for a pile of size 256. The motivation here is to see whether there is a strong correspondence to how $\tilde{h}(t; L)$ increases as a function of t during the transient. From Figure 3, we note good correspondence and conclude $\tilde{h}(t; L)$ will go as the power law in t during the transient configuration.

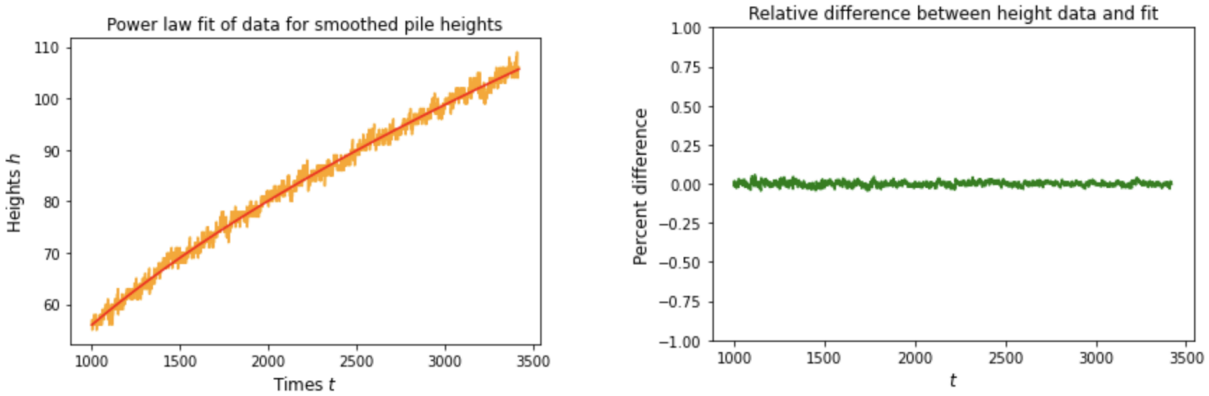

Figure 3: Left plot shows the smoothed data of pile heights fit to a power law approximation, and the right plot shows the relative difference between the data and the fit. The y-axis is scaled with range (-1, 1) corresponding to 100% deviation. We can see clearly that there is good correspondence, allowing us to conclude the transient approximates the power law in time.

2.5 Signs of corrections to scaling and parameter estimation

Let us now consider the system after it has reached the attractor of the dynamics and measure the height $h(t; L)$ for times $t \geq t_0$ where $t_0 > t_c(L)$.

We can use the average height $\langle h(t; L)\rangle_t$ to investigate corrections to scaling by calculating it at the steady state and using the following relation: $\langle h(t; L)\rangle_t = a_0 L(1 - a_1 L^{-\omega_1} + a_2 L^{-\omega_2} + ...$ where $\omega_i > 0$ and a_i are constants. We neglect the $i > 1$ terms to estimate a_0 and ω_1 using our measured data, thereby simplifying the expression to $\langle h\rangle = a_0 L\,(1 - a_1 L^{-\omega_1})$. We plot the average heights and run a non-linear least squares to fit the values and estimate the desired parameters: $a_0 = 1.764$ and $\omega_1 = 0.6126$.

2.6 Scaling behavior of $\sigma_h(L)$ with respect to L

We look at the standard deviation of the height, given by $\sigma_h(L) = \sqrt{\langle h^2(t; L)\rangle_t - \langle h(t; L)\rangle_t^2}$. When $\sigma_h(L)$ is plotted against L the result approximates a power law, and we use the familiar ansatz aL^ω with a non-linear least squares fit analysis to find $a = 0.58$ and $\omega = 0.24$. These estimates are corroborated by the results plotted in Figure 4.

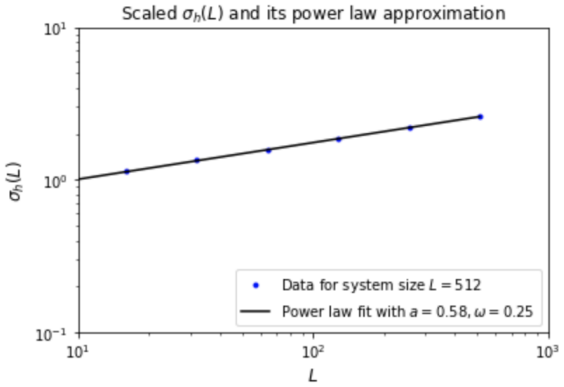

Figure 4: The standard deviation of the height for a system of size 256, $\sigma_h(L = 256)$ is plotted on a log-log plot. A power law fit with scaling parameters, estimated using a non-linear least squares fit as $a = 0.58$ and $\omega = 0.24$, is used to see how the data behaves. This provides support for using these values for the parameters in the calculations of the behavior in the limit where L tends to infinity.

From these values it is possible to estimate the behavior of the average slope and its standard deviation in the limit where L tends to infinity:

$$\lim_{L\to\infty} \langle z \rangle = a_0 = 1.764$$

$$\lim_{L\to\infty} \sigma_{\langle z \rangle} = \lim_{L\to\infty} \sigma_{\frac{\langle h \rangle}{L}} = \lim_{L\to\infty} (\sigma_h \cdot \frac{1}{L}) = \lim_{L\to\infty} (0.58 \cdot L^{0.24} \cdot \frac{1}{L}) = 0.58 \cdot \lim_{L\to\infty} L^{-0.76} = 0$$

2.7 Considerations of height probabilities

2.7.1 Statistical theory

Assuming the local slopes are independent, identically-distributed random variables with finite variance we expect $P(h; L)$ to follow a Gaussian (normal) distribution [2] about the mean $\langle h \rangle$, and that this distribution can be scaled by multiplying by $\sigma_h(L)$. Here, $\sigma_h(L)$ will equal the square root of the variance. This can be written as $z_i \sim N(\langle h \rangle, \sigma_h^2(L))$ and expressed

$$P(h; L) = \frac{1}{\sigma_h \sqrt{2\pi}} e^{-\frac{1}{2}\left(\frac{h - \langle h \rangle}{\sigma_h}\right)^2}$$

2.7.2 Data collapse of measured height probability $P(h; L)$

We now plot $P(h; L)$ against h and use the measured values of $\langle h \rangle$ and σ_h to produce a data collapse. Specifically, we transform the distributions along the h-axis by negative $\langle h \rangle$ and a multiple of $L^{-0.24}$, and along the P-axis by a multiple of $L^{0.24}$. As a result, the set of distributions now share an average mean $\langle h \rangle = 0$ and a standard deviation of $\sigma_h = 1$. The transformation can be related to the original distribution by a scaling function $\mathcal{F}\prime$ where

$$P(h; L) = \frac{1}{\sigma_h} \mathcal{F}\prime \left(\frac{h - \langle h \rangle}{\sigma_h} \right) \Rightarrow \mathcal{F}\prime x = \frac{1}{\sqrt{2\pi}} e^{-\frac{1}{2}(x)^2} \tag{4}$$

2.7.3 Analysis of theoretical function and numerical test

Yes, the data collapse traces out a Gaussian distribution as was predicted. The implication here is that the local slopes are indeed independent and identically-distributed random variables.

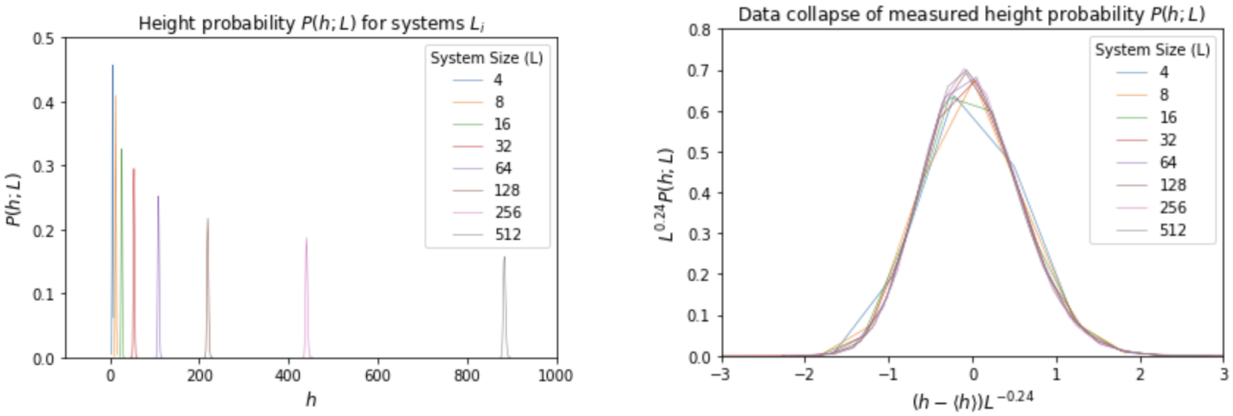

Figure 5: The height probabilities for various systems are plotted before and after data collapse to a scaling function $\mathcal{F}\prime$. The result is a Gaussian distribution with $h = 0$ and $\sigma_h = 1$, which agrees with our theoretical prediction for the case of independent, identically-distributed random variables with finite variance.

Also, that the system self-organizes around a critical point driven by the standard deviation and the mean of the height probability.

Our numerical test involves plotting larger system size in the data collapse so as to achieve a Gaussian distribution. This is successful for a system of size 512, which can be seen graphed against the other system sizes in Figure 5. It is also possible to calculate numerically and plot the difference between our measured data and a Gaussian. This would be useful for revealing any correlation between the local slopes that we have taken to be 0 in our work.

3 The avalanche-size probability $P(s;L)$

We turn our focus to measuring avalanche-size probability $P(s;L)$ and associated moments k_i. Consider a steady-state system of size L and define avalanche size s as the number of relaxations triggered by adding a single grain at site $i = 1$.

3.1 Plotting normalized avalanche-size probability

The plot of avalanche-size probabilities $\tilde{P}_N(s;L)$ against avalanche size s can be seen in Figure 6. N is chosen to be $N = 10^6$ to be large enough such that the cutoff effect is clearly visible. The data is log-binned because the variables are not continuous and produce a sparse tail. This leads to noise in the model. The procedure for log-binning is described in [3] and can be expressed by

$$\tilde{P}_N\left(s^j\right) = \frac{\text{No. of avalanches in bin } j}{N\Delta s^j} \tag{5}$$

for $s^j = \sqrt{s^j_{\min} s^j_{\max}}$ where s^j is the geometric mean of the avalanche sizes in bin j.

The distribution for $\tilde{P}_N(s;L)$ follows a power law trend with no characteristic length s. Each system size has a cutoff avalanche size s_c after which the system's avalanche-size probability experiences a steep drop. Larger system sizes generally have larger avalanche-sizes, but even for $L = 256$ there is a cutoff point after which the probability of having a large avalanche is negligible. This cutoff goes as roughly $s_c \propto L^2$, which is in agreement with our ansatz, $s_c = L^{2.25}$. The little uptick seen in Figure 7 is typical and due to a finite-size effect which disappears in the infinite limit of L, and the avalanche-size probability scales as the power law: $P(s;L) \propto s^{-\tau_s}$.

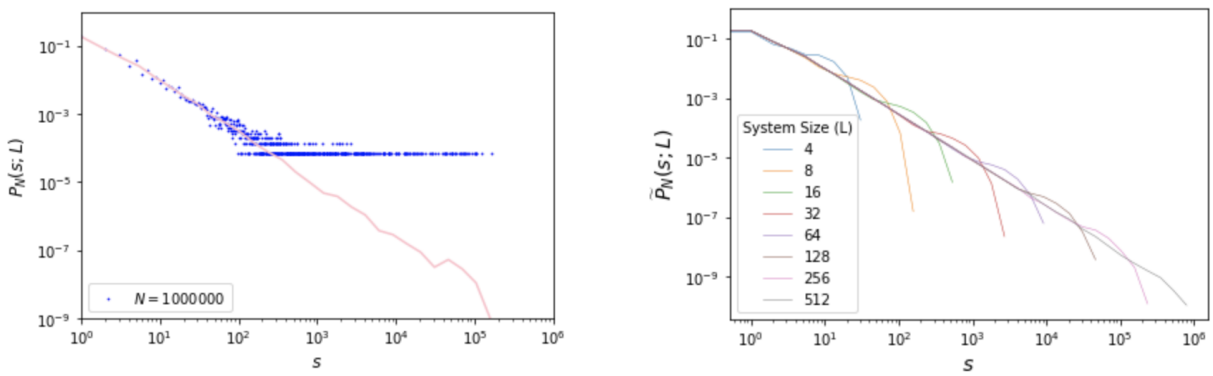

Figure 6: Data is log-binned with scale 1.2 to show the cut-off avalanche size s_c. The normalized probability heights are then plotted for all system sizes L_i over $N = 10^6$ iterations. It is easy to see the curve for $L = 256$, shown in pink on both plots. On the right plot, all system sizes are plotted and the s_c visible for each. We note there is no characteristic avalanche size.

3.1.1 Finite-size scaling ansatz

We perform a data collapse and use it to estimate avalanche dimension D and avalanche-size exponent τ_s. Since we saw before the avalanche-size scales as L^D, we divide by a factor of L^D along the s-axis. The resulting distribution is translated along the P-axis by multiplying by a factor of s^{τ_s}. This is motivated by the fact that $P(s;L) \propto s^{\tau_s}$. Combining these transformations, we find a scaling function $\mathcal{G}$ that satisfies the finite-scaling ansatz

$$\tilde{P}_N(s;L) \propto s^{-\tau_s}\mathcal{G}\left(s/L^D\right) \qquad \text{for } L \gg 1, s \gg 1 \tag{6}$$

From here we are able to estimate $D = 2.25$ and $\tau_s = 1.55$ for $L \ll 1$, $s \ll 1$. As we go to the limit where L is sufficiently large, we would expect finite-size effects to be negligible and there would not be a small uptick as is seen in Figure 7. This uptick is interesting, however, as it suggests that in the finite case we would see more avalanches than expected around the cutoff size, and that this behavior would vanish for the infinite case.

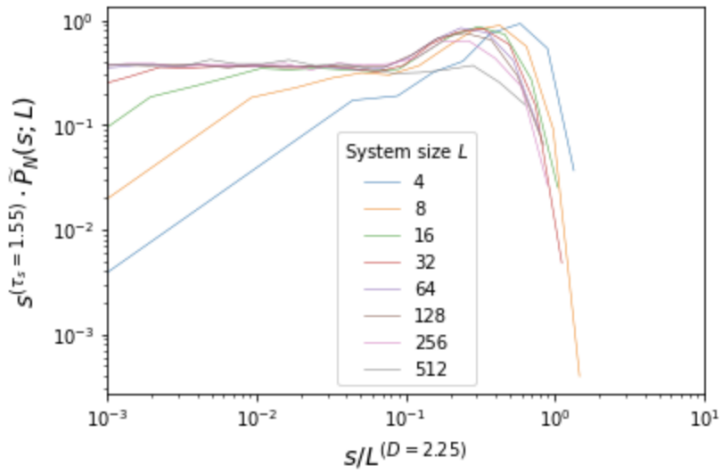

Figure 7: The data is collapsed using a scaling function $\mathcal{G}$ and the associated relation in Equation 6. That is, the axes were scaled in accordance with the underlying power law $P(s;L) \propto s^{-\tau_s}$. Values for avalanche dimension $D = 2.25$ and avalanche-size exponent $\tau_s = 1.55$, are calculated by running an optimized least-square regression. There is obviously a mistake here, and fixing it is left as an exercise to the grader.

3.2 Measuring directly the kth moment $\langle s_k \rangle$

We now wish to directly measure the kth moment of the avalanche-size probability, $\langle s^k \rangle = \sum_{s=1}^{\infty} s^k \tilde{P}(s;L)$ for k =1, 2, 3, 4 where s_t is the measured avalanche size at time t, $t_0 > t_c(L)$. Though avalanches of size 0 are included in the normalized probability, their contribution to the sum is identically 0. However, we retain our assumption that $L \gg 1$. We proceed:

$$\begin{aligned}
\langle s^k \rangle &= \sum_{s=1}^{\infty} s^k \tilde{P}_N(s;L) \\
&= \sum_{s=1}^{\infty} s^{k-\tau_s} \mathcal{G}\left(\frac{s}{L^D}\right) \\
&\approx \int_1^{\infty} s^{k-\tau_s} \mathcal{G}\left(\frac{s}{L^D}\right) ds \\
&= \int_{1/L^D}^{\infty} \left(uL^D\right)^{k-\tau_s} \mathcal{G}(u) du \\
&= L^{D(1+k-\tau_s)} \int_{1/L^D}^{\infty} (u)^{k-\tau_s} \mathcal{G}(u) du \\
&\propto L^{D(1+k-\tau_s)} = L^{\phi} \quad \text{for } L \gg 1
\end{aligned} \tag{7}$$

From this, we can infer the kth moment exhibits scaling behavior as would be expected of a self-organized system. In particular, the exponent has a linear dependence on k and from this relationship it is possible to infer the values of the parameters.

We find a linear relationship between the scaling exponent ϕ and moment k, and compute the parameters of the linear function. We can now write $\phi = 2.27k - 1.27$, and check our previous work in estimating D and τ_s, assuming without loss of generality that $k = 1$:

$$L^{D(1+k-\tau_s)} = L^{\phi} \Rightarrow D(1+k-\tau_s) = \phi = 2.27k - 1.27 \tag{8}$$

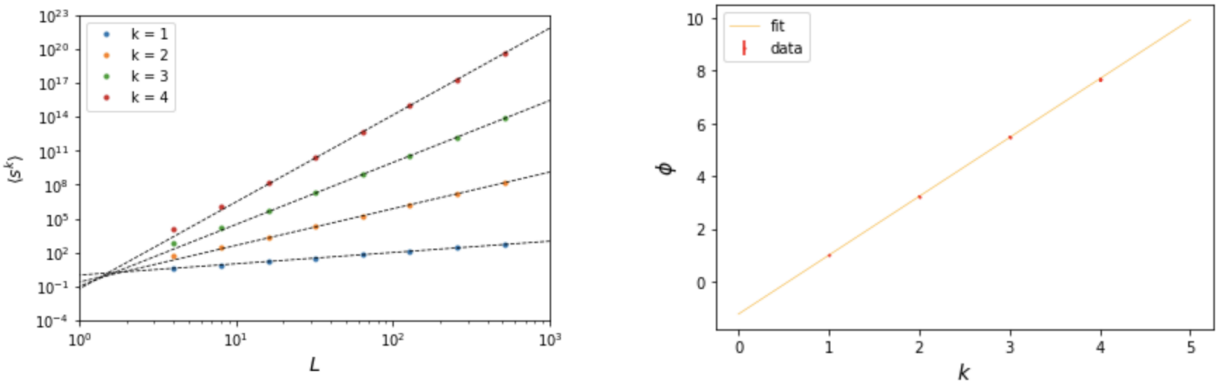

Figure 8: The kth moments are plottee against system size and a least squares regression run to show the fit is a reasonable one. The linear relation for ϕ in Equation 8 is plotted with error bars, which start very small and increase slightly.

4 Conclusions

In this report, we have examined the scaling behavior characteristic of the Oslo model to better understand self-organized criticality. We generated piles over a range of system sizes to see how these would behave relative to each other, but also to see whether and how they would collapse with a scaling function.

The behavior of the pile height $h(t; L)$ was studied through its average and found to collapse onto a scaling function $\mathcal{F}(x)$. We saw that in a steady-state configuration, $h(L) \propto L$ and $\langle t_c(L) \rangle \propto L^2$. This was confirmed with both theoretical argument and numerical calculation.

Finally, avalanche-size probabilities were found to go as the power law. From this, the parameters of avalanche-size dimension D and avalanche-size exponent τ_s were estimated, and later verified using a relation from the data collapse analysis. This brought us to verifying the kth moments of the avalanche size obeyed the finite-size scaling ansatz. In this step, the separation of time scales that is characteristic of avalanches was clear from the drive and duration on the plotted results.

The Oslo model proved to be an illuminating example of self-organized criticality, and displayed all the expected signs of such a complex system; namely, scaling and data collapse.

References

[1] D. Dhar, *Steady State and Relaxation Spectrum of the Oslo Rice-pile model*, Physica A **340**, 535 (2004).

[2] A.T Adeniran and O. Faweya. *Derivation of Gaussian Probability Distribution: A New Approach*, Applied Mathematics, 11, 436-446. 2020.

[3] K.Christensen and N.Maloney, *Complexity and Criticality*, Imperial College Press, London, 2005.